STRUCTURAL BEHAVIOUR OF HIGH STRENGTH CONCRETE COLUMNS REINFORCED WITH GLASS FIBRE REINFORCED POLYMER BARS UNDER AXIAL LOADING

SASIKUMAR P* , MANJU R
Department of Civil Engineering, Kumaraguru College of Technology, Coimbatore-641049, Tamil Nadu, India

The present study carried out the axial compressive behaviour of High Strength Concrete (HSC) columns reinforced with GFRP bars under axial compression. Only a limited number of research works only done with GFRP Reinforced (RC) Concrete Columns. Twelve columns of 150x150mm cross-section and 1000mm height made with M70 grade of HSC, including 1.20% of Alkaline Resistant Glass Fibre (AR-GF), were tested under axial loading. The main parameters were studied in this research, including the Axial Load (AL) carrying capacity, axial deformation, failure pattern, ductility, and stiffness. GRFP RC columns are 90% axial load only carried compared to steel RC columns. The analytical study helped to predict the ultimate AL carrying capacity of HSC columns.

Keywords: *High strength concrete, Axial load, Axial deformation, Stiffness, Ductility, GFRP bars*

1. Introduction

In recent decades RC structures have been mainly affected by corrosion in severe environmental conditions. It's causing a loss of strength and efficiency. Several studies have been conducted to increase concrete strength and solve corrosion problems. High-strength concrete is promoted to use in the construction industry in a wide range. HSC has more advantages compared to normal-strength concrete. Its HSC is more durable, and the designer minimises the cross-section area of the element. On the industrial side, they are developing high-strength concrete made by alternative reinforcement with non-corroding GFRP bars. Reinforcement concrete structures completed HSC with GFRP bars, increasing the service life of the structural elements.

RC structures exposed to harsh environmental conditions are plagued by corrosion of the steel reinforcement. The steel reinforcing is being replaced with new materials and has been studied to solve the steel corrosion problem [1]. Fibre Reinforced Polymers (FRP) were used as internal reinforcement for various RC structures, including bridge deck slabs, RC pavement, and coastal constructions, due to their corrosion resistance to cast with high-strength concrete [2,3]. The FRP bars were mainly used in the FRP structures for resisting tensile and flexure force, but there is a need to expand their use to include compression components that are susceptible to corrosion, such as columns. Many researchers have studied circular HSC columns by ng FRP bars under axial load [4–14]. Other researchers studied circular RC columns reinforced with FRP behaved when subjected to eccentric loads [15–17]. Only a few studies have examined eccentric and concentric loadings [18–21]. FRP was also discussed as a means of strengthening concrete columns that are rectangular or square [22–24]. Several of the experiments featured in the previous section used normal concrete, in other investigations used HSC [25,26]. Based on those investigations, a higher load capacity of columns was achieved using HSC, and more stiffeners. According to test results, the GFRP bars contributed 85 % to 90 % of AL achieved compared to RC columns.

2.Significance of research

The present research was conducted on six steel reinforced and six GFRP RC columns, out of three columns including alkaline resistant glass fibre in each group and subjected to axial loads. The experimental study results are compared with the analytical results, and the analytical results help to find out the peak AL of the columns. The comprehensive study should be as follows:

i. Studying the structural characteristics of columns with GFRP bars, to determine their mode of failure.
ii. Testing the compressive influence of GFRP bars in concrete columns.
iii. Structural behaviour HSC columns are compared in with and without AR-GF.
iv. High-strength concrete columns analyse the non-linear Finite Element Model (FEM).
v. Experimental results are compared with analytical results. Analytical results help predict the axial load of the column.

*Autor corespondent/*Corresponding author*,
E-mail: sasiserene@gmail.com

3.Experimental programme

3.1.Materials

In this research work, six HSC columns with GFRP bars, including with and without AR-GF, were prepared and tested under axial loading. All columns are made with HSC. When concrete is 28 days old, its average Compressive Strength (CS) is 78.19 N/mm^2 without AR-GF and 82.60 N/mm^2 with AR-GF. Three columns were prepared without AR-GF, and the remaining columns were designed with AR-GF.

3.2.GFRP bars

The ribbed GFRP bars are used to make HSC columns, as shown in Fig. 1, the ribbed bars are used in column longitudinal and transverse directions, and their high bonding strength surrounds the concrete. The mechanical properties of the GFRP bars are listed in Table 1.

3.3.Steel reinforcement

The deformed bar Fe 500 grade was used in this work, 12mm for longitudinal and 8mm transverse reinforcement, respectively. These steel bars were tested, and their mechanical properties are presented in Table 1.

Fig. 1 - GFRP bars

3.4. Properties of concrete

All specimens were made of HSC with a water-binding ratio of 0.26. The cement was used in Ordinary Portland Cement (OPC) 53 grade. The concrete inclusion of mineral admixture silica fume and fly ash 10% by mass of cement. When adding the 1.20% AR-GF to the concrete, the strength of the concrete is increased compared to the control sample. The three cube specimens were tested on the same day the columns were tested. The concrete mix properties are list out in Table 2.

3.5. Preparation of specimens

Table 3 summarises the details of six columns. The first part of the work was to prepare the GFRP reinforcement and ties. In the GFRP reinforcement cage model shown in Fig. 2, the bars were cut 950mm in length, the links were placed 100mm centre to centre, and it is tightly biding by using binding wire, finally aligned in a steel mould. The oil was placed in the inner portion of the steel mould. The oil is prevented adhesive to the steel mould and concrete. The high-strength concrete is placed on the steel mould, and the concrete is compacted uniformly throughout the entire length using a needle vibrator. On the same day, three cubes are cast in each mix with and without AR-GF. The steel mould was removed after 24 hours, and the columns were cured in 28 days. The column was tested after the curing period.

3.6.Specimen setup and instrumentation

The specimens were tested after the curing period in the loading frame capable of 200 T under the AL, as shown in Fig. 3. The samples were placed in the vertical direction under the loading frame. Specimens were aligned in the centre position to carry the axial load. The bottom portion of the sample was placed on a rigid base; a 10 mm thick plate was placed in the bottom and top portions of the specimens. Two LVDTs were set to measure the column's lateral deflection, and the remaining one was placed in the vertical direction to measure the axial deformation of the specimen.

Table 1

GFRP bars properties

S.No	Bar type	Dia of bar	Area of bar	Tensile strength in N/mm^2	Young's Modulus in GPa	Strain
1	GFRP	12	78.13	890	42	0.020
2	GFRP	8	50.26	750	42	0.022
3	Steel	12	78.13	500	200	0.002
4	Steel	8	50.26	500	200	0.002

Table 2

High strength concrete mix proportions

S. No	Materials	kg/m^3
1	Cement	419.20
2	Fly ash	52.40
3	Silica fume	52.40
4	Fine aggregate	595
5	Coarse aggregate	1228
6	Superplasticizer	6.29
7	Water	138
8	W/B ratio	0.26

Table 3

Specimen details

Specimen ID	Specimen dimensions (mm)			Longitudinal reinforcement	Transverse reinforcement
	B	D	L		
RCC1-1	150	150	1000	4 No. #12mm	#8mm @ 100c/c
RCC1-2	150	150	1000	4 No. #12mm	#8mm @ 100c/c
RCC1-3	150	150	1000	4 No. #12mm	#8mm @ 100c/c
RCC2-1	150	150	1000	4 No. #12mm	#8mm @ 100c/c
RCC2-2	150	150	1000	4 No. #12mm	#8mm @ 100c/c
RCC2-3	150	150	1000	4 No. #12mm	#8mm @ 100c/c
GFRP1-1	150	150	1000	4 No. #12mm	#8mm @ 100c/c
GFRP1-2	150	150	1000	4 No. #12mm	#8mm @ 100c/c
GFRP1-3	150	150	1000	4 No. #12mm	#8mm @ 100c/c
GFRP2-1	150	150	1000	4 No. #12mm	#8mm @ 100c/c
GFRP2-2	150	150	1000	4 No. #12mm	#8mm @ 100c/c
GFRP2-3	150	150	1000	4 No. #12mm	#8mm @ 100c/c

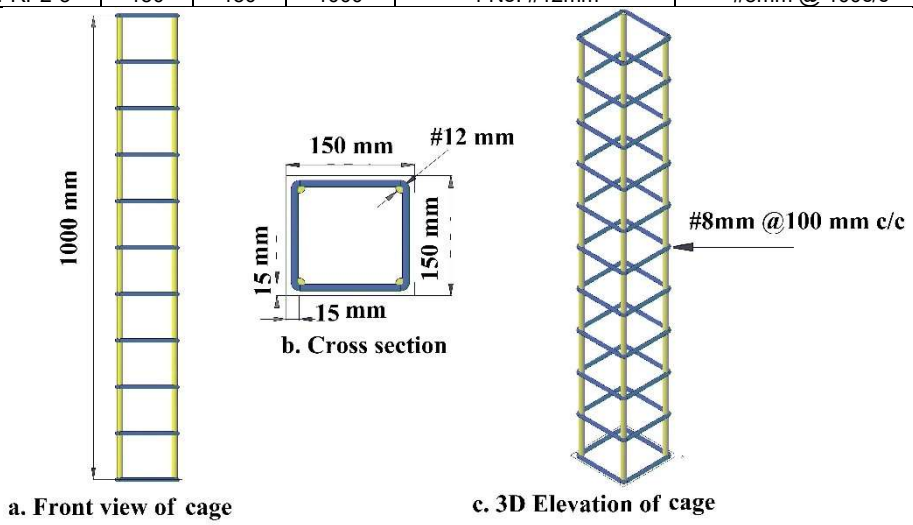

Fig. 2 - Geometry properties

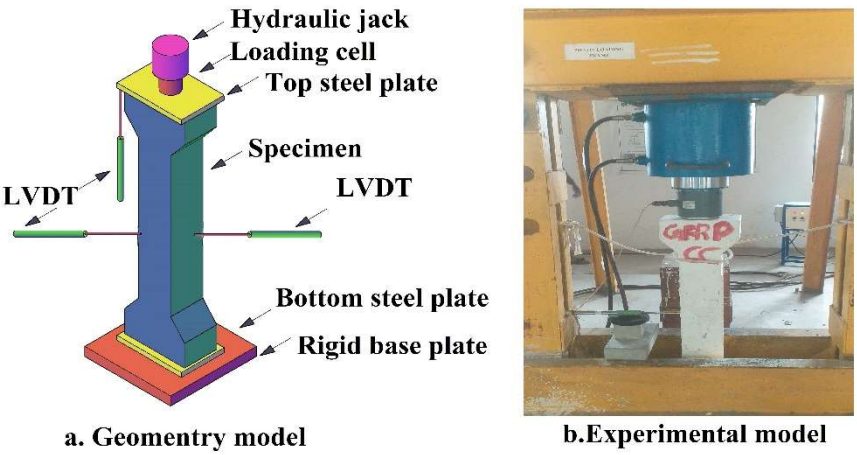

Fig. 3 - Specimen setup and instrumentation

4. Analytical work

4.1.Finite Element Model (FEM)

The FEM was developed in Ansys. FEM helps predict the ultimate AL and failure of the specimens.

4.2. Mesh

The high-strength concrete columns are considered in three parts steel cage, high-strength plain cement concrete, and high-strength RC columns, as shown in Fig. 4. The HSC columns are analysed FEM using Ansys software. Three types of mesh are used in this work fine, medium, and large; based on the analytical study, and large mesh helps predict the ultimate axial load of the column, as shown in Fig. 5.

4.3.Axial load-deformation in finite element model

Fig. 6 was shown the boundary condition of the HSC column. The HSC columns are analysed in Ansys software. The load is applied in the vertical direction axially. The column specimen is considered bottom is fixed and top-hinged

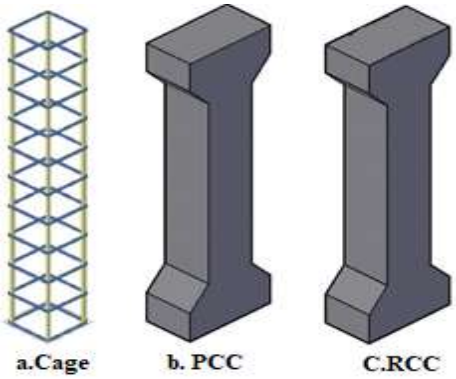

Fig. 4 - Components of high strength concrete column

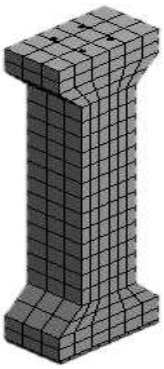

Fig. 5 - Mesh of high strength concrete column

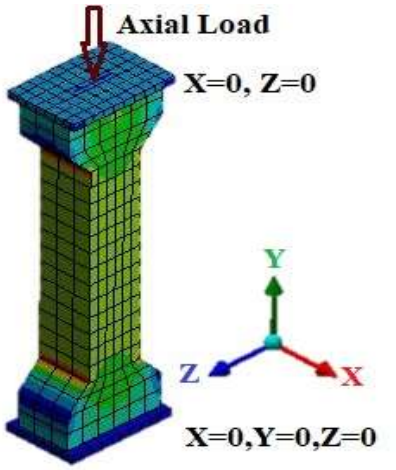

Fig. 6 - Loading condition of column

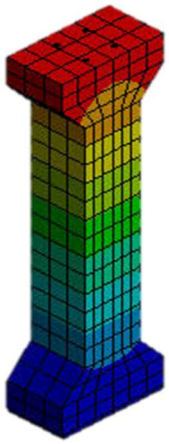

Fig. 7 - Axial deformation of the column

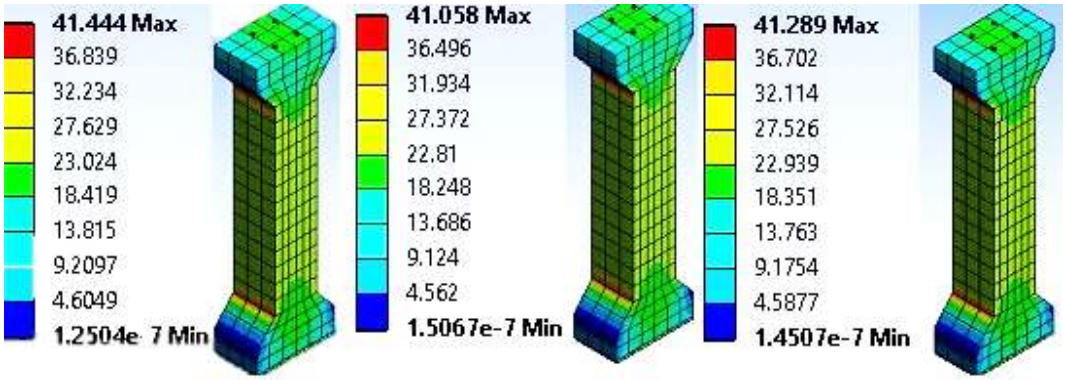

Fig. 8 - Stress behaviour under axial load in RCC1 (1-3) columns

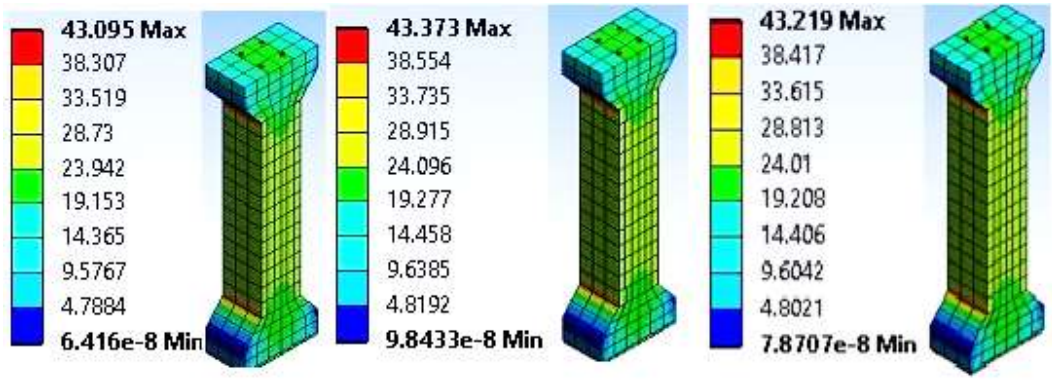

Fig. 9 - Stress behaviour under axial load in RCC2 (1-3) columns

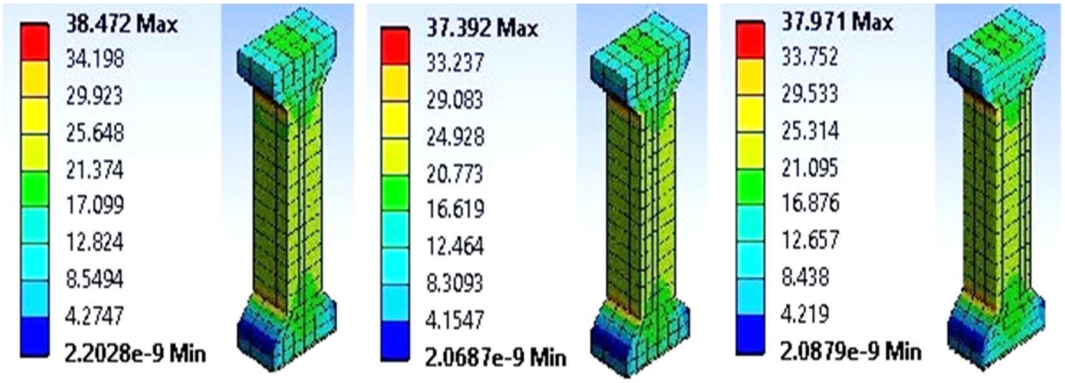

Fig. 10 - Stress behaviour under axial load in GFRP1 (1-3) columns

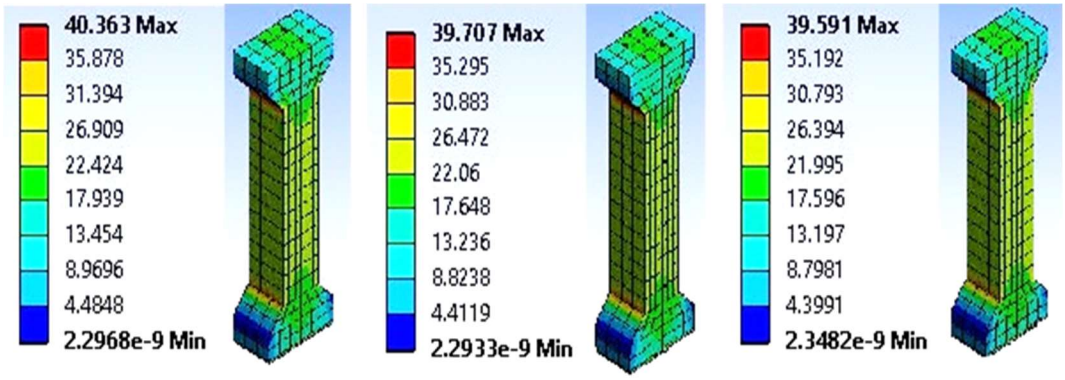

Fig. 11 - Stress behaviour under axial load in GFRP2 (1-3) columns

condition, and the maximum axial deformation in the top portion is shown in Fig. 7. The axial stress distribution of all columns is shown in Figs. 8-11.

5.Results and discussion

5.1.Axial Load Capacity (ALC) of columns

The columns are divided into four groups, the first two groups are RCC, and the remaining two groups are GFRP, each group cast with and without AR-GF. Each group has three specimens (RCC1-1, RCC1-2, RCC1-3, RCC2-1, RCC2-2, RCC2-3, GFRP1-1, GFRP1-2, GFRP1-3, GFRP2-1, GFRP2-2, GFR2-3) are tested under axial loading as shown in Figs. 12-13. A GFRP RC column is designed with axial load capacity determined by the concrete regarding the cross-section area column, and the role of the GFRP bars has yet to be discovered by CSA [27], and ACI since no experiments have been conducted [28]. Throughout the literature, various authors have shown that GFRP longitudinal bars are crucial for accurately predicting the ALC of concrete columns [4,5,19,22]. Due to the different failure modes, it was difficult to determine the exact ALC of the GFRP bars in concrete columns. Afifi et al.[4] where required for the CS of GFRP bars, as shown in Eq. (1). GFRP bars compressive strength is calculated according to Tobbi et al.[22] linear-elastic theory using the 2000 με Eq. (2). Although this model indicates a strain level lower than that measured in the experiment, and it produces a predicted load more down than the actual load measured in the investigation. Samani and Attard [29] suggested that the axial strain level for unconfined concrete strength for cylinders was (ε_{FRP}) 2500 με Eq. (3). Based on the experimental study, axial load up to 61% was only achieved for the above three equations, and Eq. (4) was given better results for both steel and GFRP RC columns. Although according to ACI [30], the concrete area contributed approximately 0.85 of the concrete CS.

$$P_n = 0.85 \times f_c \times (A_g - A_{FRP}) + 0.35 \times f_{u\,FRP} \times A_{FRP} \quad (1)$$

$$P_n = 0.85 \times f_c \times (A_g - A_{FRP}) + 0.002 \times E_{FRP} \times A_{FRP} \quad (2)$$

$$P_n = 0.85 \times f_c \times (A_g - A_{FRP}) + 0.0025 \times E_{FRP} \times A_{FRP} \quad (3)$$

$$P_P = A_c P_{ck} + A_s P_{sk} \quad (4)$$

Where:
$P_{ck} = 0.4\ (f_{ck})$ and
$P_{sk} = 0.67 f_y$

Where A_c and A_g refer to the area of concrete; A_s refer to the area of longitudinal reinforcement of bar; P_{ck} and fc refer to the CS of concrete; P_{sk} refers to yield strength of longitudinal reinforcement bar; E_{FRP} and $A_{FRP,}$ which represents the modulus of elasticity and cross-sectional area of the FRP longitudinal reinforcement; $f_{u\ FRP}$ which means the ultimate tensile strength of the GFRP bar.

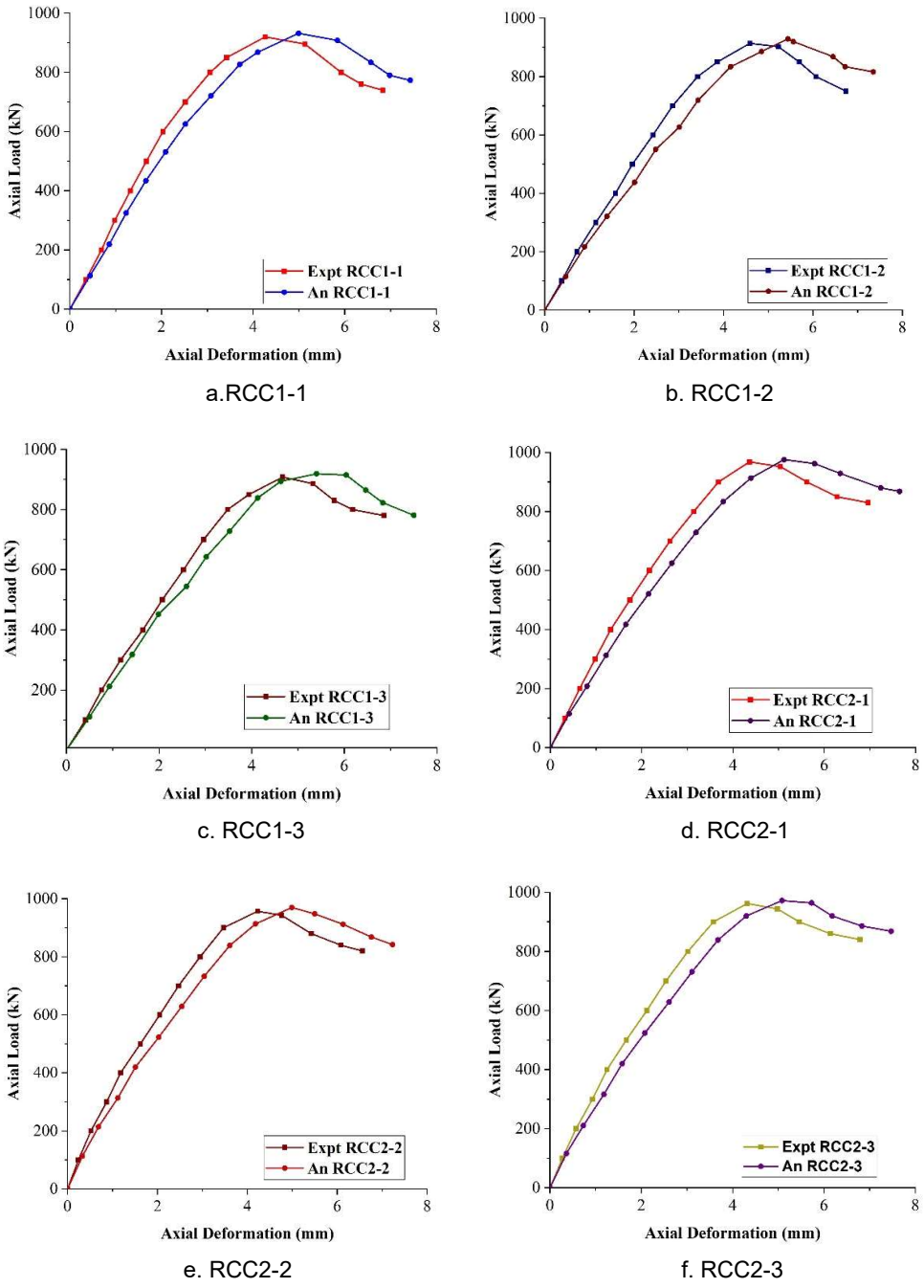

a.RCC1-1 b. RCC1-2

c. RCC1-3 d. RCC2-1

e. RCC2-2 f. RCC2-3

Fig. 12 - Axial load-deformation response for column groups RCC1&2

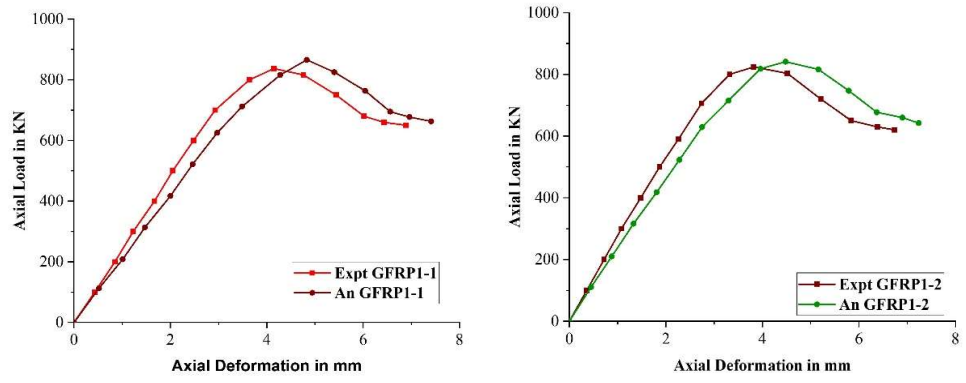

a.GFRP1-1 b. GFRP1-2

Fig.13 continues on next page

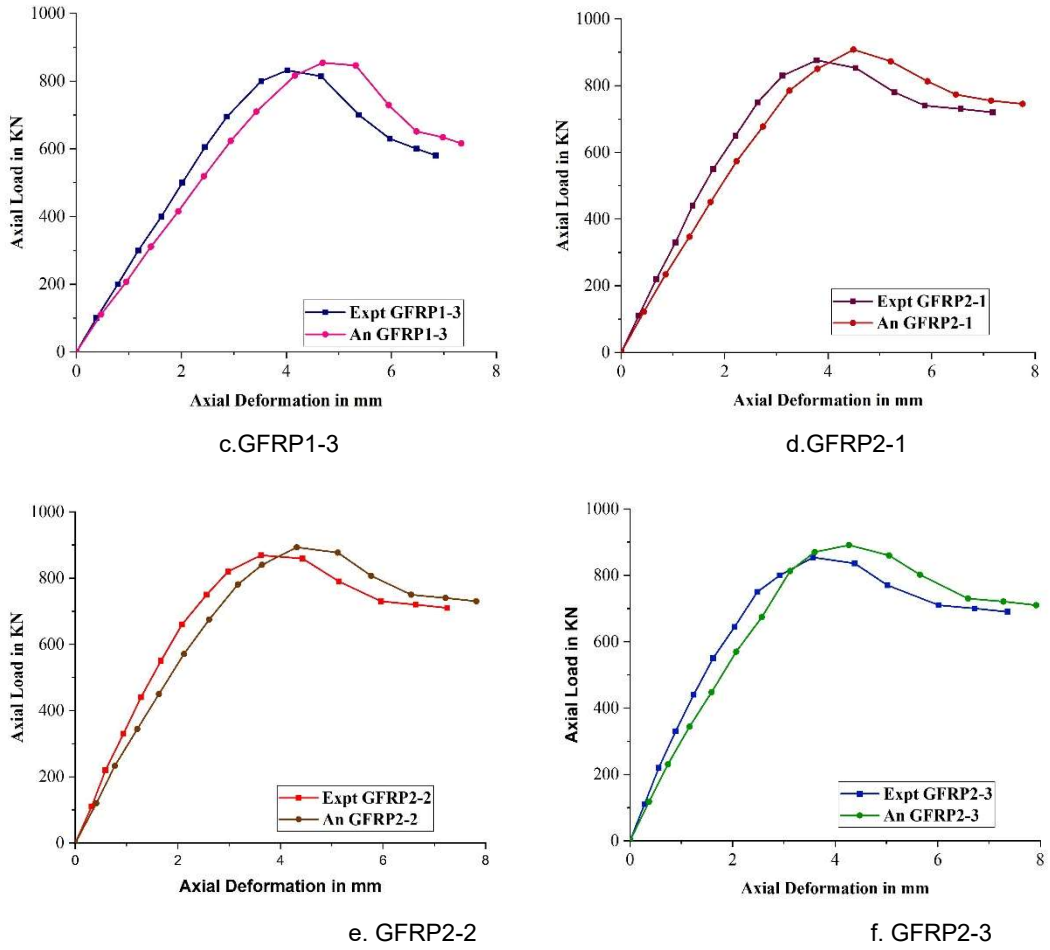

Fig. 13 - Axial load-deformation response for column groups GFRP1&2

Table 4

Comparison between experimental and design load

Specimen ID	Experimental load (kN)	Eq. (1)	Eq. (2)	Eq. (3)	Eq. (4)
RCC1-1	920	0.61	0.60	0.60	1.08
RCC1-2	914	0.61	0.60	0.59	1.07
RCC1-3	908	0.60	0.59	0.59	1.06
RCC2-1	968	0.61	0.60	0.59	1.08
RCC2-2	957	0.60	0.59	0.59	1.07
RCC2-3	962	0.60	0.59	0.59	1.07
GFRP1-1	837	0.55	0.56	0.56	0.86
GFRP1-2	824	0.54	0.55	0.55	0.85
GFRP1-3	832	0.55	0.56	0.55	0.86
GFRP2-1	876	0.55	0.55	0.55	0.87
GFRP2-2	869	0.54	0.55	0.55	0.86
GFRP2-3	854	0.53	0.54	0.54	0.85

Table 4 lists the difference between the calculated ALC and that measured experimentally (P_n) by calculated with Eqs. (1 - 3), which ranged from 39 to 46%. As a result, Eq. (4) was able to provide a good match between axial capacity prediction results based on test results [31].

5.2.Mode of failure

A failure mode of the tested HSC columns is shown in Fig. 14. A hairline crack develops at the bottom of all tested specimens, causing failure to commence. With increasing the load, the cracks grew, widened, and propagated along with the bottom and top portion of the column. This was observed by failure mode, crack pattern, concrete cover spalling, buckling of vertical reinforcement and tie reinforcement, and crushing of concrete core. RCC1 columns are failed concrete crushing, concrete cover spalling, and longitudinal failure. RCC2 is almost the exact failure behaviour, but the columns failed without concrete cover spalling. In the GFRP1 and GFRP2 column groups, failure is noted during testing. GFRP1 column groups failed with widened cracks and concrete cover spalling, but GFRP2 column groups failed in local buckling behaviour and buckling of the longitudinal bar. The experimental and analytical results are summarised in Table 5.

a.RCC1 b.RCC2 c.GFRP1 d.GFRP2

Fig. 14 - failure of RCC and GFRP columns

Table 5

Comparison between yield, ultimate, and failure load

ID	Yield load (kN)		Ultimate load (kN)		Failure load (kN)		Mode of failure
	Expt	An	Expt	An	Expt	An	
RCC1-1	700	721	920	932	896	908	CCS
RCC1-2	692	728	914	919	902	915	CCS + CC
RCC1-3	703	719	908	929	886	920	CS + CC
RCC2-1	710	729	968	976	952	962	CC + FP
RCC2-2	724	733	957	970	943	948	CC + SF
RCC2-3	715	724	962	972	944	964	CC + FP
GFRP1-1	600	625	837	866	816	825	CC +CCS
GFRP1-2	590	629	824	841	803	816	CC +SF
GFRP1-3	605	623	832	854	814	848	CC
GFRP2-1	650	644	876	908	853	873	CC+SF
GFRP2-2	660	675	869	893	859	877	CC+SF
GFRP2-3	645	674	854	891	836	860	CC+CC

*CCS; Concrete Cover Spalling: CC; Concrete Crushing: FP; Fibre Pull out: SF; Sudden Failure

The failure pattern of all columns is noted, and the column groups of GFRP1 and GFRP2 had low axial load-carrying capacity compared to the RCC1 and RCC2 columns groups. Also, tests of all columns were compared with the analytical model, as shown in Fig. 15.

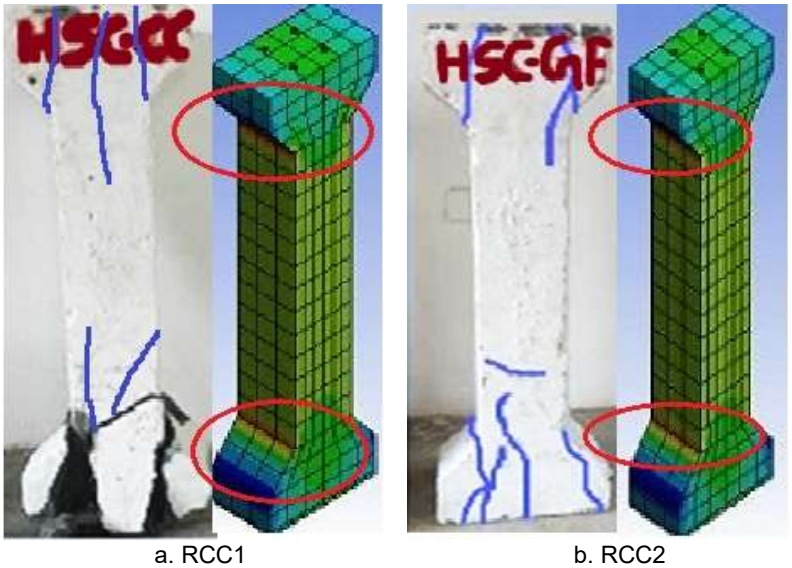

a. RCC1 b. RCC2

Fig. 15 continues on next page

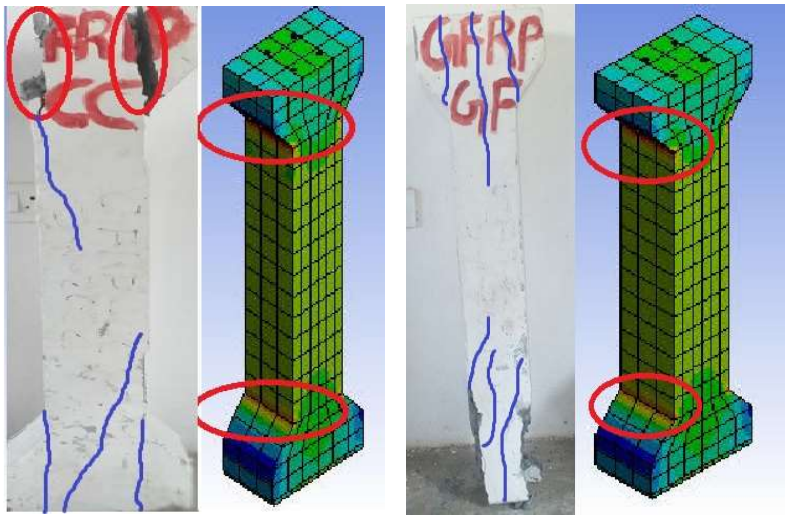

c. GFRP1 d. GFRP2

Fig. 15 - Comparison of experimental and analytical failure mode in all columns

Table 6

Comparison between experimental and analytical loads

ID	Experimental load (kN)	Analytical load (kN)
RCC1-1	920	932
RCC1-2	914	919
RCC1-3	908	929
RCC2-1	968	976
RCC2-2	957	970
RCC2-3	962	972
GFRP1-1	837	866
GFRP1-2	824	841
GFRP1-3	832	854
GFRP2-1	876	908
GFRP2-2	869	893
GFRP2-3	854	891

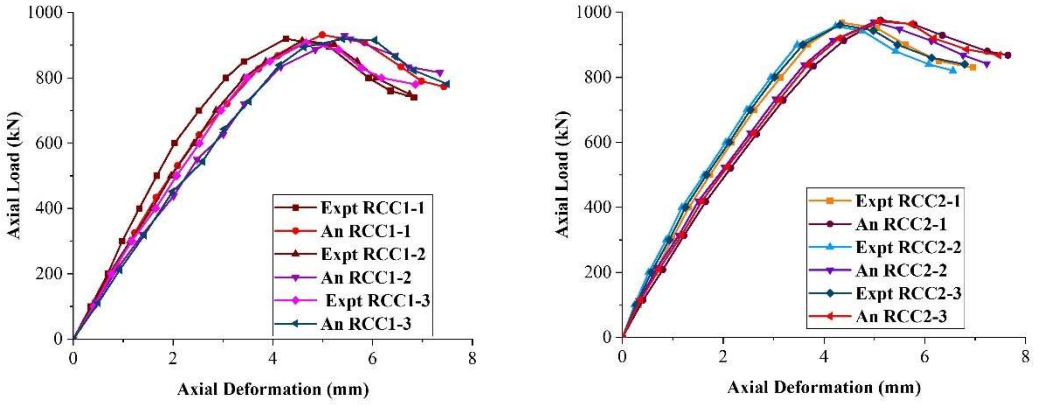

a.RCC1 b. RCC2

Fig.16 - Axial load-deformation response in column groups RCC 1&2

5.3.Comparison between experimental and analytical results

The HSC columns tested under AL, RCC1, and RCC2 are maximum AL compared to the GFRP1 and GFRP2 columns. GFRP columns achieved only 85 to 90 % axial load compared to RCC columns, and analytical results help predict the ultimate load, as listed in Table 6. The axial load-deformation curves are shown in Figs.16-17, and average axial load-deformation behaviour is shown in Fig.18.

5.4.Ductility

Fig. 19 illustrates that columns that use GFRP bars exhibit a three-phase response to axial loads. There are no cracks in a column at the beginning, which is determined by a linear elastic limit. As a result of hairline cracks propagating during axial deformation Δ_1, nonlinear behaviour was observed (P_y). In other words, P_y is the maximum load tolerated by the concrete, and longitudinal reinforcement before the outer concrete cover completely erodes. A drop in load occurred

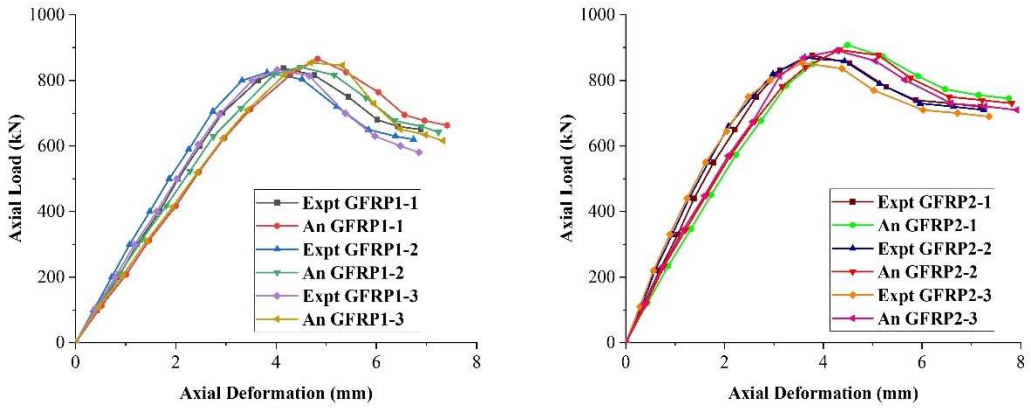

c. GFRP 1 d. GFRP 2

Fig.17 - Axial load-deformation response in column groups GFRP 1&2

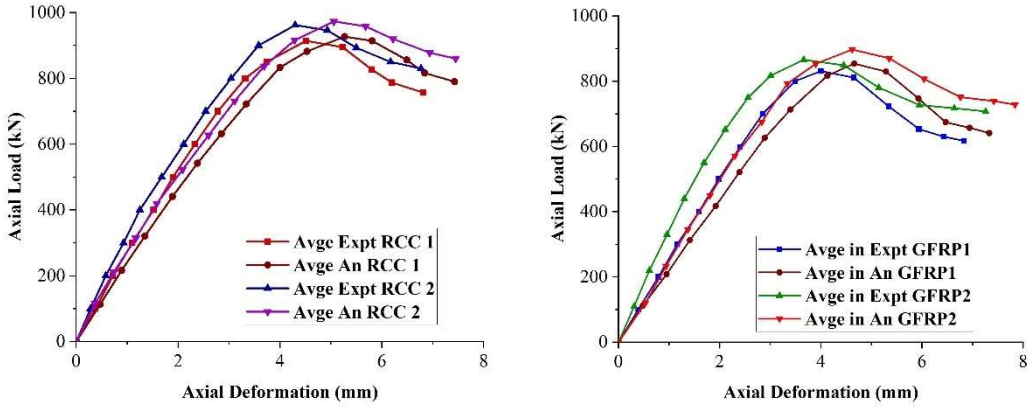

a. RCC1&2 b. GFRP1&2

Fig. 18 - Average axial load-deformation response in column groups RCC&GFRP

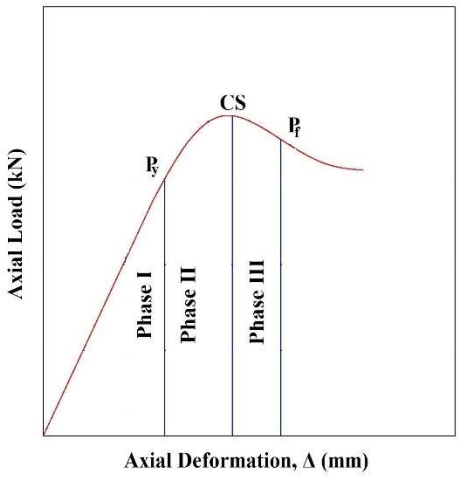

Fig. 19 - Axial load-deformation curve

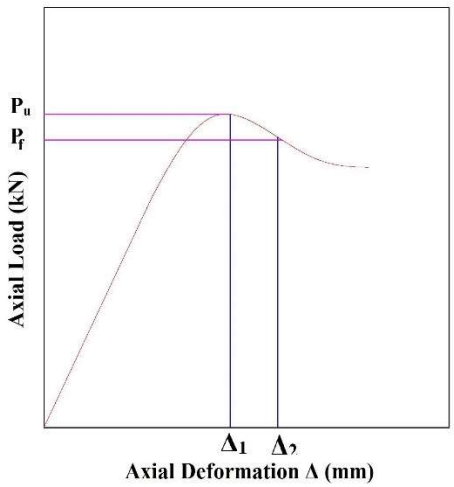

Fig. 20 - Ductility factor for columns

during the second phase due to cracks in the concrete cover, which also contributed to greater concrete Cover Spalling (CS). The effective column area was reduced at this stage. The concrete cover has been completed or partially spalled during phase three. Therefore, if the concrete core is confined laterally, the applied load can increase the deformation as the failure load (P_f) increases. It is considered as the failure load of the specimen and mentions axial deformation by Δ_2.

To be durable, an object must be able to withstand plastic deformation before it fails [32]. Table 7 compared GFRP-reinforced HSC columns to RCC columns based on their behaviour to determine their ductility and stiffness. The ductility is higher compared to the AR-GF in steel and GFRP column groups. Meanwhile, ductility is lower

Table 7

Comparison between experimental and analytical ductility and stiffness

ID	Yield load (kN)		Deformation at yield point (mm)		Deformation at failure point (mm)		Ductility factor (μ_Δ)		Stiffness (k) (kN/mm)	
	Expt	An	Expt	An	Expt	An	Expt	An	Expt	An
RCC1-1	700	721	2.52	3.08	5.13	5.84	2.04	1.90	281.75	234.09
RCC1-2	692	728	2.86	3.40	5.23	5.60	1.83	1.65	241.26	214.12
RCC1-3	703	719	2.96	3.52	5.32	6.04	1.80	1.72	238.18	204.26
RCC2-1	710	729	2.62	3.19	5.04	5.73	1.92	1.80	267.18	228.53
RCC2-2	724	733	2.47	3.04	4.76	5.50	1.93	1.81	277.33	241.12
RCC2-3	715	724	2.54	3.11	4.98	5.79	1.96	1.86	273.23	235.05
GFRP1-1	600	625	2.48	2.97	4.76	5.40	1.92	1.82	241.94	210.44
GFRP1-2	590	629	2.26	2.75	4.52	5.16	2.00	1.88	261.06	228.73
GFRP1-3	605	623	2.45	2.94	4.66	5.32	1.90	1.81	246.94	211.90
GFRP2-1	650	644	2.21	2.74	4.53	5.21	2.05	1.90	294.12	235.04
GFRP2-2	660	675	2.08	2.61	4.43	5.12	2.13	1.96	317.31	258.62
GFRP2-3	645	674	2.04	2.57	4.38	5.05	2.15	1.96	316.18	262.26

compared to without AR-GF in both groups. the GFRP bars columns failed 85 - 90% axial load compared to the RCC columns. The ductility factor (DF) μ_Δ was calculated by Eq. (5) as the ratio between ultimate axial deformation to failure axial deformation, as shown in Fig. 20.

$$\mu_\Delta = \frac{\Delta 2}{\Delta 1} \quad (5)$$

6.Conclusions

This work was carried out as an experimental and analytical study of the HSC column with GFRP bars under axial compression inclusion with and without AR-GF. The results of the experimental and analytical tests can be summarised as follows:

- Steel-reinforced HSC columns and GFRP-reinforced HSC columns performed similarly. Steel RC columns failed due to concrete crushing, but GFRP RC columns failed suddenly after peak load because GFRP bars broke along with concrete crushing.
- The peak load was experienced by most of the tested columns. The ultimate and failure loads of both steel and GFRP RC columns (P_u and P_f) were noted.
- There were approximately constant loads on the steel- RC columns after the ultimate load while axial deformations increased. After the ultimate load, however, GFRP RC columns developed continuous increases in load with increasing axial deformations to failure.
- The ultimate load was higher when AR-GF was added; however, when the GFRP RC columns were increased. Additionally, the GFRP RC columns were better suited for ductile failure.
- In the case of GFRP-reinforced HSC columns, most showed gradual failures with higher axial deformations and better ductility than steel-reinforced HSC columns.
- Comparison with steel-reinforced HSC columns, the GFRP bars only carried between 85% to 90 % of the axial load.
- According to the tests, equations are used to predict the strength of confined concrete. Results from experiments are compared to the equations. Although Eq.4 only gave better predictions, it helps compare experimental and analytical test results.
- The analytical model and experimental curves showed reasonable correlations for the axial load deformation. At the post-peak stage, however, there were significant deviations.
- The study concluded that GFRP bars could effectively replace steel reinforcement in cases where corrosion risk exists.
- Inclusion of AR-GF in steel-RC columns and GFRP RC columns failed without concrete cover spalling and increased axial load.
- FEM analyses help predict tested specimens AL carrying capacity and compare them with experimental results.

REFERENCES

[1] M. Elchalakani, M. Dong, A. Karrech, M.S. Mohamed Ali and J.S. Huo, Circular concrete columns and beams reinforced with GFRP bars and spirals under axial, eccentric, and flexural loading, J. Compos. Constr., 2020, **24**, 04020008.

[2] K. Bouguerra, E.A. Ahmed, S. El-Gamal and B. Benmokrane, Testing ofarisons full-scale concrete bridge deck slabs reinforced with fiber-reinforced polymer (FRP) bars, Constr. Build. Mater., 2011, **25**, 3956–3965.

[3] B. Benmokrane, E. El-Salakawy, A. El-Ragaby and S. El-Gamal, Performance evaluation of innovative concrete bridge deck slabs reinforced with fibre-reinforced-polymer bars, Candian J. Civ. Eng., 2007, **34**, 298–310.

[4] M.Z. Afifi, H.M. Mohamed and B. Benmokrane, Axial Capacity of Circular Concrete Columns Reinforced with GFRP Bars and Spirals. J. Compos. Constr., 2014, **18**, 04013017.

[5] G.B. Maranan, A.C. Manalo, B. Benmokrane, W. Karunasena and P. Mendis, Behavior of concentrically loaded geopolymer-concrete circular columns reinforced longitudinally and transversely with GFRP bars, Eng. Struct., 2016, **117**, 422–436.

[6] M.N.S. Hadi, W. Wang and M.N. Sheikh, Axial compressive behaviour of GFRP tube reinforced concrete columns, Constr. Build. Mater., 2015, **81**, 198–207.
[7] H.A. Hasan, M.N. Sheikh and M.N.S. Hadi, Maximum axial load carrying capacity of Fibre Reinforced-Polymer (FRP) bar reinforced concrete columns under axial compression, Struct., 2019, **19**, 227–233.
[8] C.P. Pantelides, M.E. Gibbons and L.D. Reaveley, Axial load behavior of concrete columns confined with GFRP spirals, J. Compos. Constr., 2013, **17**, 305–313.
[9] H.M. Mohamed, M.Z. Afifi and B. Benmokrane, Performance Evaluation of Concrete Columns Reinforced Longitudinally with FRP Bars and Confined with FRP Hoops and Spirals under Axial Load, J. Bridge Eng., 2014, **19**, 04014020.
[10] H. Karim, M.N. Sheikh and M.N.S. Hadi, Axial load-axial deformation behaviour of circular concrete columns reinforced with GFRP bars and helices, Constr. Build. Mater., 2016, **112**, 1147–1157.
[11] H. Tobbi, A.S. Farghaly and B. Benmokrane, Behavior of concentrically loaded fiber-reinforced polymer reinforced concrete columns with varying reinforcement types and ratios, ACI Struct. J., 2014, **111**, 375–385.
[12] N.A. Farhan, M.N. Sheikh and M.N.S. Hadi, Behaviour of ambient cured steel fibre reinforced geopolymer concrete columns under axial and flexural loads, Struct., 2018, **15**, 184–195.
[13] B. Vijaya, S.S. Selvan and P. Vasanthi, Experimental investigation on the behaviour of reinforced concrete column containing manufactured sand under axial compression, Mater. Today Proc., 2020, **39**, 446–453.
[14] O.S. AlAjarmeh, A.C. Manalo, B. Benmokrane, W. Karunasena, P. Mendis and K.T.Q. Nguyen, Compressive behavior of axially loaded circular hollow concrete columns reinforced with GFRP bars and spirals, Constr. Build. Mater., 2016, **194**, 12–23.
[15] X. Fan and M. Zhang, Behaviour of inorganic polymer concrete columns reinforced with basalt FRP bars under eccentric compression: An experimental study, Compos. Part B Eng., 2016, **104**, 44–56.
[16] K. Khorramian and P. Sadeghian, Experimental and analytical behavior of short concrete columns reinforced with GFRP bars under eccentric loading, Eng. Struct., 2017, **151**, 761–773.
[17] A. Salah-Eldin, H.M. Mohamed and B. Benmokrane, Structural performance of high-strength-concrete columns reinforced with GFRP bars and ties subjected to eccentric loads, Eng. Struc., 2019, **185**, 286–300.
[18] M.N.S. Hadi and J. Youssef, experimental investigation of gfrp-reinforced and gfrp-encased square concrete specimens under axial and eccentric load, and four-point bending test. J. Compos. Constr., 2016, **20**, 04016020.
[19] M.N.S. Hadi, H. Karim and M.N. Sheikh, Experimental investigations on circular concrete columns reinforced with gfrp bars and helices under different loading conditions, J. Compos. Constr., 2016, **20**, 04016009.
[20] A. Hadhood, H.M. Mohamed and B. Benmokrane, Experimental Study of Circular High-Strength Concrete columns reinforced with GFRP bars and spirals under concentric and eccentric loading, J. Compos. Constr., 2017, **21**, 04016078.
[21] A. Raza, Q. uz and Z. Khan, Structural behavior of GFRP-reinforced Circular HFRC columns under concentric and eccentric loading, Arabian J. Science Eng., 2021, **46**, 4239–4252.
[22] H. Tobbi and A.S. Farghaly, B. Benmokrane, Concrete columns reinforced longitudinally and transversally with glass fiber-reinforced polymer bars. ACI Struct. J., 2012, **109**, 551–558.
[23] A. De Luca, F. Matta and A. Nanni, Behavior of full-scale GFRP reinforced concrete columns under axial load, ACI Struct. J., 2010, **105**, 1-31
[24] M.A. Ali, E. El-Salakawy, seismic performance of gfrp-reinforced concrete rectangular columns, J. Compos. Constr., 2016, **20**, 04015074.
[25] T.A. Hales, C.P. Pantelides and L.D. Reaveley, Experimental evaluation of slender high-strength concrete columns with GFRP and hybrid reinforcement, J. Compos. Constr., 2016, **20**, 04016050.
[26] A. Hadhood, H.M. Mohamed and B. Benmokrane, Strength of circular HSC columns reinforced internally with carbon-fiber-reinforced polymer bars under axial and eccentric loads, Constr. Build. Mater., 2017, **141**, 366–378.
[27] CSA (2012), Design and construction of building structures with fibre-reinforced polymers.
[28] ACI (2015), Guide for the design and construction of concrete reinforced with FRP bars, (ACI), Farmington. Hills, Mich., USA.
[29] A.K. Samani and M.M. Attard, A stress-strain model for uniaxial and confined concrete under compression, Eng. Structr., 2012, **41**, 335–349.
[30] ACI (2008), Building code requirements for structural concrete (ACI 318-08) and commentary.
[31] IS 456 (2000), Plain Concrete and Reinforced, Indian Standard. Dehli.
[32] G.P. Lignola, F. Nardone, A. Prota, A. De Luca and A. Nanni, Analysis of RC hollow columns strengthened with GFRP, J. Compos. Constr., 2011, **15**, 545–556.

****